Journal of the European Ceramic Society 21 (2001) 2759–2763

www.elsevier.com/locate/jeurceramsoc

Effect of sintering process on microstructure characteristics of $Ba(Mg_{1/3}Ta_{2/3})O_3$ ceramics and their microwave dielectric properties

Mei-Hui Liang[a], Chen-Ti Hu[a], Hsiu-Fung Cheng[b], I-Nan Lin[c,*], John Steeds[d]

[a]*Department of Materials Science and Engineering, National Tsing-Hua University, Hsinchu, Taiwan 300, ROC*
[b]*Department of Physics, National Taiwan Normal University, Taipei, Taiwan, ROC*
[c]*Materials Science Center, National Tsing-Hua University, Hsinchu, Taiwan 300, ROC*
[d]*Department of Physics, University of Bristol, Bristol BS8 1TL, UK*

Abstract

Microstructure of $Ba(Mg_{1/3}Ta_{2/3})O_3$, BMT, materials were examined using transmission electron microscopy. Selected area electron diffractions imply that the ordering of Mg^{2+} and Nb^{5+} cations transforms the BMT materials from cubic symmetry to $P\bar{3}m1$ symmetry, which induces the formation of polar domains in BMT grains. Large grains contain wavy polar domain boundaries, dislocations and even the dislocation networks, which are detrimental to the microwave dielectric properties. Presumably, induction of abundant defects in association with large BMT grains is the prime factor degrading the microwave dielectric properties of the BMT materials, when they were sintered at too high temperature.

Keywords: $Ba(Mg_{1/3}Ta_{2/3})O_3$; Microwave dielectrics; TEM microstructure

1. Introduction

In consonance with the technological development trends in the miniaturization of microwave communication circuits, the development of high-performance dielectric materials is urgently needed. Perovskite $Ba(Mg_{1/3}Ta_{2/3})O_3$, BMT materials, which contain Mg- and Ta-ions arranged in an ordered fashion, possess the highest Q-factor ($Q \times f \cong 35{,}000$ GHz at 10 GHz) among the known microwave dielectric materials and thus have great potential for application to devices.[1–2] However, the sintering conditions required to achieve high performance for BMT materials in very stringent.[3–7] The mechanism involved is still not well understood[8–16]. To understand how does the processing parameters influence the microwave characteristics of BMT materials, the microstructure of these materials were examined using transmission electron microscopy.

2. Experiments

The perovskite $Ba(Mg_{1/3}Ta_{2/3})O_3$, BMT, powders were synthesized by a two-step process, in which $MgTa_2O_6$ powders were first prepared by the mixed oxide process and were then mixed with $BaCO_3$ in a 1:3 molar ratio for nominal composition $Ba(Mg_{1/3}Ta_{2/3})O_3$, followed by calcination at 800 °C. Thus obtained BMT powders were then pelletized and sintered at 1450–1650 °C for 4 h. The crystal structure and the microstructure of the sintered BMT samples were examined by X-ray diffraction analysis (XRD, Rigaku D/max-IIB) and scanning electron microscopy (SEM, Joel JSM-840A), respectively. The microwave dielectric properties were measured using H.P.8722A network analyzer in a resonant cavity or parallel plate test fixture. The defects in the materials were examined using transmission electron microscopy.

3. Results and discussion

High-density BMT materials (~95.5%T.D.) can be obtained by sintering the 2-step calcined BMT powders, which are of pure perovskite structure (bottom XRD pattern, Fig. 1a), at 1550 °C for 4 h. Variations of

* Corresponding author. Tel.: +886-3-5742574; fax: +886-3-5716977.
E-mail address: inlin@mx.nthu.edu.tw (I.-N. Lin).

0955-2219/01/$ - see front matter
PII: S0955-2219(01)00359-4

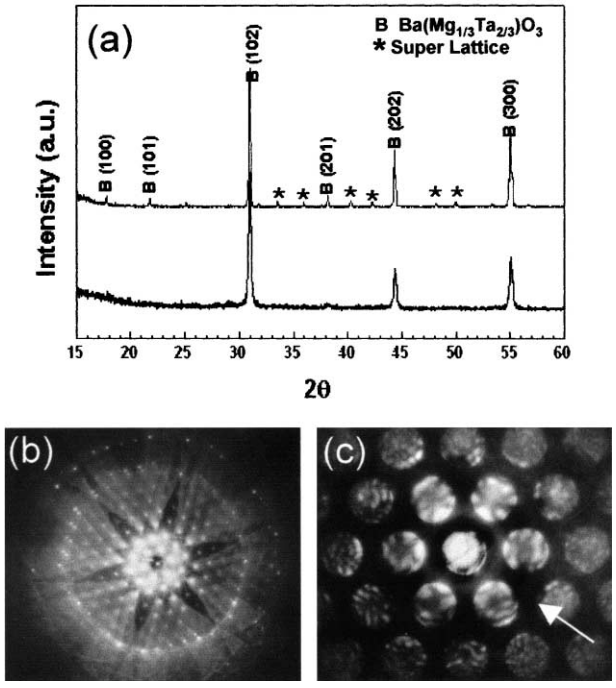

Fig. 1. (a) Typical X-ray diffraction (XRD) patterns, (b) conventional electron diffraction pattern along $<111>$ axis and (c) convergent beam electron diffraction patterns along $<111>$ axis for $Ba(Mg_{1/3}Ta_{2/3})O_3$ materials; in (a), the bottom XRD pattern represents the 800 °C-calcined, whereas the top XRD pattern represents the 1550 °C×4 h sintered BMT materials.

microwave dielectric properties of the BMT materials with the sintering temperature are illustrated in Table 1, indicating that although the samples were maintain at the same high density ($\geqslant$95.5%T.D.), the quality factor ($Q\times f$-value) of the materials decreases monotonously as the sintering temperature increases from 1550 to 1650 °C. No secondary phase was induced for high temperature sintered samples. Therefore, the probable cause of deterioration is presumed to be the induction of the defects. Microstructure examination using transmission electron microscopy is thus performed.

Typical X-ray diffraction patterns of high-density BMT materials is shown in Fig. 1a (top XRD pattern), indicating that the materials are perovskite with $a_0 = 5.782$ nm. High degree of ordering occurs, as indicated by the presence of satellite diffraction peaks. However, detailed analyses using selected area diffraction (SAD) in TEM illustrate that, although the zeroth order Laue zone (0th-LZ) for (111)-zone of BMT materials possesses 6-fold symmetry, the first order Laue zone (1st-LZ) owns only one mirror plane symmetry (Fig. 1b). Such a phenomenon is even more clearly illustrated by the convergent beam electron diffraction (CBED) patterns in Fig. 1c, where the mirror plane was indicated by an arrow. These results reveal that the ordered materials are not of cubic symmetry. One of the $<111>$ axis is stretched due to the ordering of Ta^{5+} and Mg^{2+} cations, resulting in a structure with lower symmetry, viz. $P\bar{3}m$, which is in accord with previous reports[16].

Only the $<111>$ axis containing stretching direction of Ta^{5+}–O–Mg^{2+} chains possess 6-fold symmetry, which is designated as polar axis. The other $<111>$ axes possess only mirror plane. Deviation of such a distorted lattice from cubic is so small that X-ray diffraction analysis cannot clearly differentiate the quasi-cubic structure from the true cubic one. Even the electron diffraction analysis in TEM needs special technique such as CBED to unambiguously resolve the *polar axis* from non-polar axis. There are 4 possibilities for the *polar axis* in the BMT lattices, i.e. $<111>$, $<11\bar{1}>$, $<1\bar{1}1>$ and $<\bar{1}11>$ directions. The BMT grains are separated into several *polar domains*, which are the regions with polar axis oriented in the same direction. It should be noted that *polar domains* are resulted only when the Ta^{5+} and Mg^{2+} cations are ordered. The polar domain boundaries are totally different from the anti-phase boundary, in which the sequence of arrangement for the two Ta^{5+}-ions and Mg^{2+}-ions along the same polar axis changes.

Typical TEM micrograph of BMT materials are illustrated in Fig. 2, showing that the grains are smaller (~0.75 μm) for BMT materials sintered at 1550 °C×4 h (Fig. 2a) and are larger (~2.4 μm) for those sintered at 1650 °C×4 h (Fig. 2b). The grain size distribution is very uniform for both materials. Most of the grains contain wavy contrast, probably the boundaries of polar domains. In fine grain BMT materials (1550 °C-sintered), large grains occur occasionally. Fig. 3a illustrates a typical example, where a large grain about 1.5 μm in size was surrounded by the small grains, which are ~0.75 μm. It is interesting to observe that the large grains contain 4 sub-regions (labeled as a_1, a_2, a_3 and a_4) separated by sharp boundaries. Diffraction analysis indicates that the 4 sub-regions are actually belonging to the same grains. The contrast in the 4 sub-regions implies that they are of slightly different diffraction conditions. Probably, the large grain is formed by merging 4 adjacent small grains, a_1–a_4, with each grain slightly tilted and having its polar axis oriented in different $<111>$ direction. A large grain containing 4 polar domains is thus resulted. The boundary between

Table 1
Variation of microwave dielectric properties of BMT materials with sintering conditions (the BMT powders were prepared by two-step calcinations process)

Sintering conditions	Density (%T.D.)	Dielectric constant	Quality factor ($Q\times f$)(GHz)	τ_f (ppm/°C)
1500 °C×4 h	95.5	24	400,000	8.13
1550 °C×4 h	95.0	25	600,000	8.13
1600 °C×4 h	96.0	24.5	460,000	8.13
1650 °C×4 h	95.2	24	306,000	5.14

polar domains can be straight or curves. Large proportion of strain contrast is observed at the junction of the 4 subregions, which supports the argument that large grain is resulted from the merge of adjacent small grains. The polar domain boundaries may contain dislocations, which are presumably formed to accommodate large mismatch in orientation for the original grain to merge with the large grain. Fig. 3b shows that, in some case, density of dislocation is so large that networks are developed.

Fig. 4a reveals that the grains are relatively clean, i.e. free of defects, when they are small (e.g. grain A) and contain large proportion of defects, stacking faults and dislocations, when they are large (e.g. grain B). These defects are mainly confined in the same grain. Occasionally, a large midrib is observed running across several grains (labeled as C). High-resolution image reveals that the midrib is of layer structure with lattice spacing $C_0 \cong 2.54$ nm (not shown). That the presence of defects is associated with large grains is further illustrated in Fig. 4b. Short straight stacking faults (labeled as F, Fig. 4b) are densely populated only in large grains and are hardly formed in small grains. Dislocations (labeled as C, Fig. 4b) were lined up along a band, which is actually the partial dislocations at the end of a stacking faults. The stacking faults show distinct parallel line fringes when the samples were tilted in right orientation. In the extreme case, dislocations are so dense that they tangle together, forming networks (labeled as D, Fig. 4b). Defect analysis is being undergone to identify the nature of dislocations and stacking faults.

In some cases, large inclusions surrounded by strain field are observed in extraordinarily large grains. As shown in Fig. 4c, chemical and diffraction analyses reveal that these inclusions are of the same composition and structure as the BMT materials. Usually the merge of adjacent grains will induce large strains in the vicinity of original grain boundaries. A large proportion of strains observed in Fig. 4c may be the result of the conversion of secondary particles into the perovskite. The most probable process is the transformation of $Ba_5Ta_4O_{15}$ particles into perovskite, since $Ba_5Ta_4O_{15}$ is the most

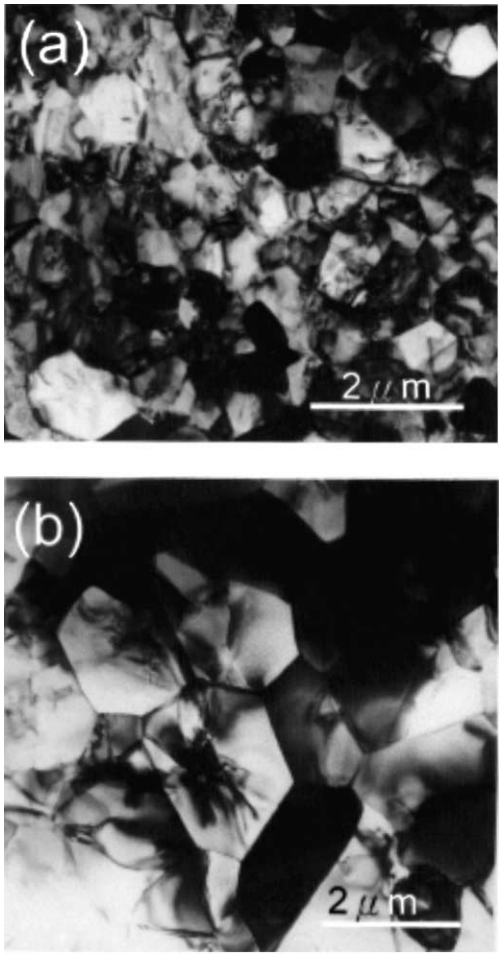

Fig. 2. Typical TEM micrographs of $Ba(Mg_{1/3}Ta_{2/3})O_3$ materials sintered at (a) 1550 °C for 4 h and (b) 1650 °C for 4 h.

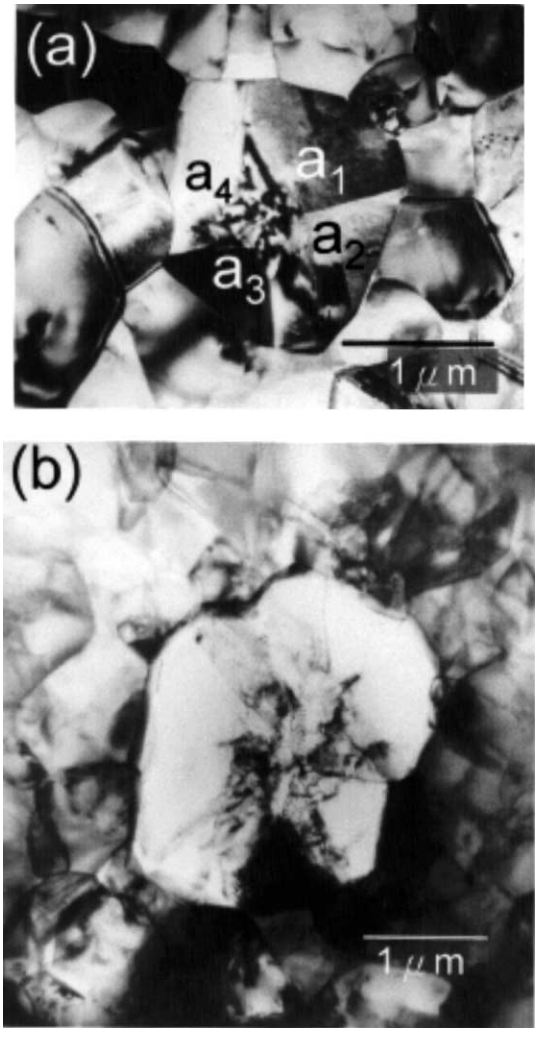

Fig. 3. (a) Micrographs of $Ba(Mg_{1/3}Ta_{2/3})O_3$ materials sintered at 1550 °C for 4 h, showing a large grain surrounded by small grains, and (b) the dislocation network near polar domain boundaries.

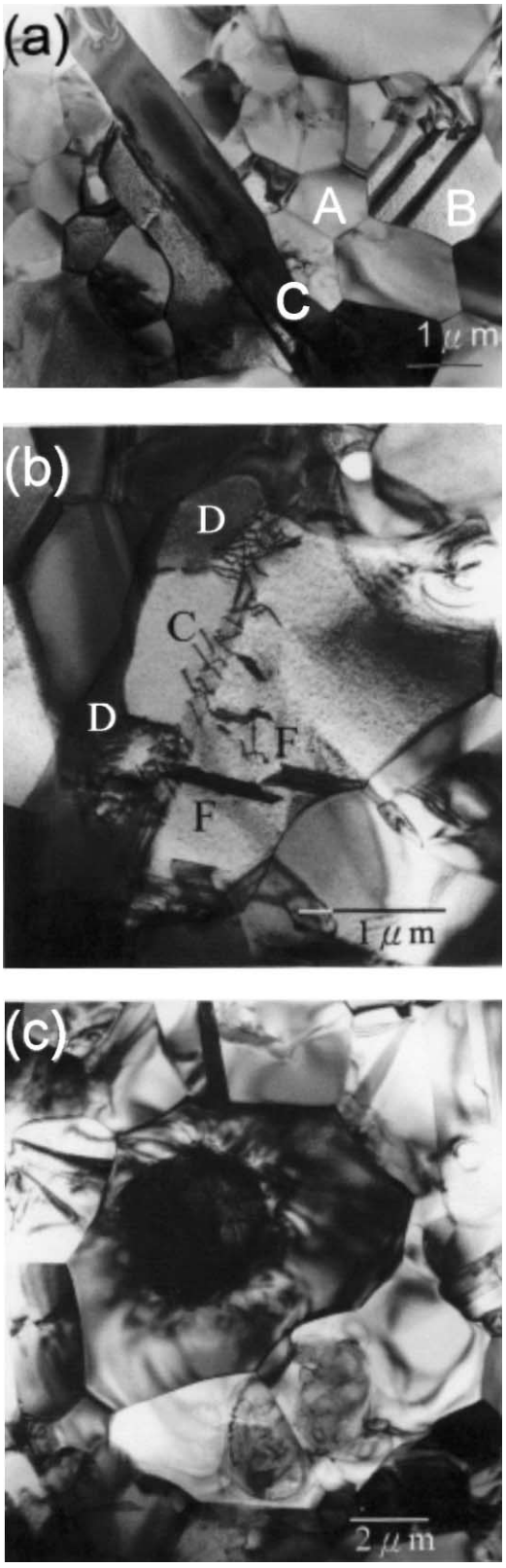

Fig. 4. (a) Typical TEM micrographs illustrates that the small grains (labeled A) are mostly defect free and the large grains (labeled B) contain large proportion of defects. Midrib (labeled C) is layered structure defects containing similar composition with BMT, frequently observed defects in large BMT grains: (b) stacking faults, F, dislocations, C, and networks, D, and (c) particle-like defects.

frequently occurring second phase formed preferentially in calcinations processes for preparing the BMT materials.

Previous results indicate that the small grains are relatively clean. Wavy contrast observed in these grains is probably the polar domain boundaries. Defects such as stacking faults and dislocations mostly occur in large grains. The presence of these kinds of defects in ceramic materials is quite unusual, since both cations and anions need to be displaced simultaneously in order to generate the dislocations and the stacking faults. Analysis on the nature of these defects is still ongoing and will be reported in the near future. However, these observations strongly imply that the presence of the defects in large BMT grains is the most probable cause degrading the microwave dielectric properties of high temperature sintered BMT materials. It should be recalled that the grain size of 1650 °C-sintered samples is about 3 times as large as that of 1550 °C-sintered ones (cf. Fig. 2). The existence of polar domain boundaries seems not to be the predominating factor degrading the microwave dielectric properties of BMT materials. Therefore, it can be concluded that suppressing the growth of grains is a possible route for improving the microwave dielectric properties of BMT materials.

4. Conclusion

The microstructure of $Ba(Mg_{1/3}Ta_{2/3})O_3$, BMT, materials was examined using transmission electron microscopy. The grains are probably growing via the merge of the adjacent grains resulting in the formation of wavy polar domain boundaries, dislocations and even the dislocation networks, which are detrimental to the microwave dielectric properties. The presence of abundant defects in large BMT grains is believed to be the prime factor degrading the microwave dielectric properties of the BMT materials sintered at a too high temperature.

Acknowledgements

The financial support of National Science Councils, ROC through project No. NSC 89-2622-E-007-005 is gratefully appreciated.

References

1. Matsumoto, H., Tamura, H. and Wakino, K., Ba(Mg,Ta)–$BaSnO_3$ high-Q dielectric resonator. *Jpn. J. Appl. Phys.,* 1991, **30**, 2347–2349.
2. Wakino, K., High frequency dielectric and their application. *IEEE Proc. 6th ISAF, 1986, 97–106.*
3. Nomura, S., Toyama, K. and Kaneta, K., $Ba(Mg_{1/3}Ta_{2/3})O_3$ ceramics with temperature-stable high dielectric constant and low microwave loss. *Jpn. J. Appl. Phys.,* 1982, **21**, L624–L626.

4. Lu, C. H. and Tsai, C. C., Reaction kinetics, sintering characteristics, and ordering behavior of microwave dielectrics: Barium magnesium tantalite. *J. Mater. Res.,* 1996, **11**, 1219.
5. Chen, X. M., Suzuki, Y. and Sato, N., Sinterability improvement of $Ba(Mg_{1/3}Ta_{2/3})O_3$ dielectric ceramics. *J. Mater. Sci.,* 1994, **5**, 244–247.
6. Nomura, S., Toyama, K. and Kaneta, K., $Ba(Mg_{1/3}Ta_{2/3})O_3$ ceramics with temperature-stable high dielectric constant and low microwave loss. *Jpn. J. Appl. Phys.,* 1982, **21**, 624–626.
7. Liang, M. H., Hu, C.T, Chiou, C. G., Tsai, Y. N. and Lin, I. N., Effect of $Ba_5Ta_4O_{15}$ incorporation on sintering behavior and microwave dielectric properties of $Ba(Mg_{1/3}Ta_{2/3})O_3$ materials. *Jpn. J. Appl. Phys.,* 1999, **38**, 71–75.
8. Galasso, F. and Pinto, J., Growth of single crystals of $Ba(B'_{0.33}Ta_{0.67})O_3$ perovskite-type compounds. *Nature, 1965, 70–72.*
9. Barber, D. J., Moulding, K. M. and Zhou, J., Structural order in $Ba(Zn_{1/3}Ta_{2/3})O_3$, $Ba(Zn_{1/3}Nb_{2/3})O_3$ and $Ba(Mg_{1/3}Ta_{2/3})O_3$ microwave dielectric ceramics. *J. Mater. Sci.,* 1997, **32**, 1531–1544.
10. Davies, P. K. and Tong, J., Effect of ordering-induced domain boundaries on low-loss $Ba(Zn_{1/3}Ta_{2/3})O_3$-$BaZrO_3$ perovskite microwave dielectrics. *J. Am. Ceram. Soc.,* 1997, **80**, 1727–1740.
11. Galasso, F. and Pyle, J., Ordering in compounds of the $A(B'_{0.33}Ta_{0.67})O_3$. *Type. J. Am. Chem. Soc.,* 1959, **81**, 482–484.
12. Tochi, K., Ohgaku, T. and Takeuchi, N., Long-wavelength phonons and effective charges in complex perovskite compounds $Ba(Mn_{1/3}Ta_{2/3})O_3$ and $Ba(Ni_{1/3}Ta_{2/3})O_3$. *J. Mater. Sci. Lett.,* 1989, **8**, 1331–1333.
13. Youn, H. J., Hong, K. S. and Kim, H., Coexistence of 1:2 and 1:1 long-range ordering types in La-modified $Ba(Mg_{0.33}Ta_{0.67})O_3$ ceramics. *J. Mater. Res.,* 1997, **12**, 589–592.
14. Youn, H. J., Kim, K. Y. and Kim, H., Microstructure characteristics of $Ba(Mg_{1/3}Ta_{2/3})O_3$ ceramics and its related microwave dielectric properties. *Jpn. J. Appl. Phys.,* 1996, **35**, 3947–3953.
15. Sagala, D. A. and Nambu, S., Microscopic calculation of dielectric loss at microwave frequencies for complex Perovskite $Ba(Zn_{1/3}Ta_{2/3})O_3$. *J. Am. Ceram. Soc.,* 1992, **75**, 2573–2575.
16. Sagala, D. A. and Koyasu, S., Infrared reflection of $Ba(Mg_{1/3}Ta_{2/3})O_3$ Ceramics. *J. Am. Ceram. Soc.,* 1993, **76**, 2433–2436.